



Performances of SMD Components on FR4 Substrates at Higher Frequencies

Veronica, Umaisaroh, Mudrik Alaydrus*

¹*Teknik Elektro, Universitas Mercu Buana,
Jl. Meruya Selatan, Jakarta 11650, Indonesia*

*Email corresponding author: mudrikalaydrus@mercubuana.ac.id

Abstract:

The advances of many technological wireless systems lead to development of several important microwave circuit components as supporting parts. The last century was the eye-witness of the development of many microwave components implemented on distributed, lumped elements or combination of them. In the design stage, we must fulfill the specified targets in terms of S-parameters over certain desired frequency intervals. The observation of several surface mounted devices installed in a microstrip structure is an important verification of the characteristics of the components especially at higher frequencies. We use the software ANSYS Electromagnetic Suite and AWR Design Environment as analytical tools. We verify the results by building the structures and measuring the reflection and transmission coefficient. The microstrip structure is modeled in a 1.4mm thick FR-4 substrate, with a dimension 50 mm x 50 mm is backed by a metallic copper ground with a thickness of 0.035 mm. We fabricated the structure under observation and did some measurement to verify its performances using a vector network analyzer. The computer programs give almost the same results for all cases except for the surface mounted device inductance. In this way we can rely on the computational modeling. The reflection and transmission coefficient of a 1.4mm thick microstrip line were verified by measurement with a very good similarity up to 5 GHz. The comparison of the simulated and measured reflection and transmission coefficient for resistor is almost the same for up to around 5 GHz, whereas for capacitor for up to around 6 GHz and for inductor for up to around 7 GHz.

Key Words:

*FR4 substrate;
High frequency;
Lumped elements;
SMD;*

Riwayat Artikel:

Received Sep 14, 2024
Revised Nov 29, 2024
Accepted Dec 05, 2024

DOI:

10.22441/incomtech.v14i3.29982

This is an open access article under the [CC BY-NC](https://creativecommons.org/licenses/by-nc/4.0/) license



1. INTRODUCTION

The advances of many technological wireless systems lead to development of several important microwave circuit components as supporting parts. The last century was the eye-witness of the development of many microwave components implemented on distributed, lumped elements or combination of them [1]. In the design stage, we must fulfill the specified targets in terms of S-parameters over certain desired frequency intervals. In order to that, there are a number of optimization methods [2], some of them involving the so-called surrogate mapping techniques and several methods from artificial intelligence [3, 4, 5].

In the past, current and future research direction, microwave filter design is still supported by representing some lumped elements as model of distributed electromagnetic structures, such as transmission lines or any discontinuities [6, 7, 8]. Even many complicated electromagnetic structures can be modeled by certain equivalent circuit, such as a highly selective and miniaturized absorption–transmission–absorption frequency-selective absorber [9] and reconfigurable metasurfaces [10].

Besides of modeling of distributed circuits, modeling and characterizing of lumped elements in a certain frequency interval got increasing attention in the previous years. In [11], a method for describing of surface-mounted device (SMD) resistor, a varactor diode, and a photo transistor in the interval of 0.5-5 GHz were proposed. Based on measurements, the authors used a Pi-model to describe the network by some lumped elements as equivalent circuit model. Many old and previous observations were documented in [12].

In [13], an impedance measurement fixture is designed. The deembedded measured S parameters are compared with the results obtained by full-wave calculation. A detailed observation on SMD resistor was carried out by modeling the SMD resistor precisely [14]. The obtained reflection coefficient was used for deriving parasitic elements for external and internal parts of the SMD resistor. In [15] an approach based on S parameter and IP-encrypted 3D model libraries for full-wave electromagnetic simulation was proposed.

In this work, we observe the characteristics of several SMD components embedded in microstrip transmission lines at higher frequencies. We compared the reflection and transmission coefficient of the SMDs obtained by computer simulations and measurements.

2. RESEARCH METHOD AND COMPUTATION MODEL

The observation of several surface mounted devices (SMD) installed in a microstrip structure is an important verification of the characteristics of the components especially at higher frequencies. Here, we use the software ANSYS Electromagnetic Suite 19.2.0/HFSS [16] and AWR Design Environment v22.1 [17] as analytical tools. We verify the results by building the structures and measuring the reflection and transmission coefficient.

The microstrip structure is modeled in a 1.4mm thick FR-4 substrate, which has a relative permittivity of 4.4 and a dielectric loss tangent of 0.02. According to TX Line tool, we choose the strip width 2.82 mm in order to get a characteristic

impedance 50 ohm. Figure 1 on the left side shows the HFSS model. The FR4 substrate with a dimension 50 mm x 50 mm is backed by a metallic copper ground with a thickness of 0.035 mm, the strip has a dimension 50 mm x 2.82 mm, whose ends are defined as port 1 and port 2.

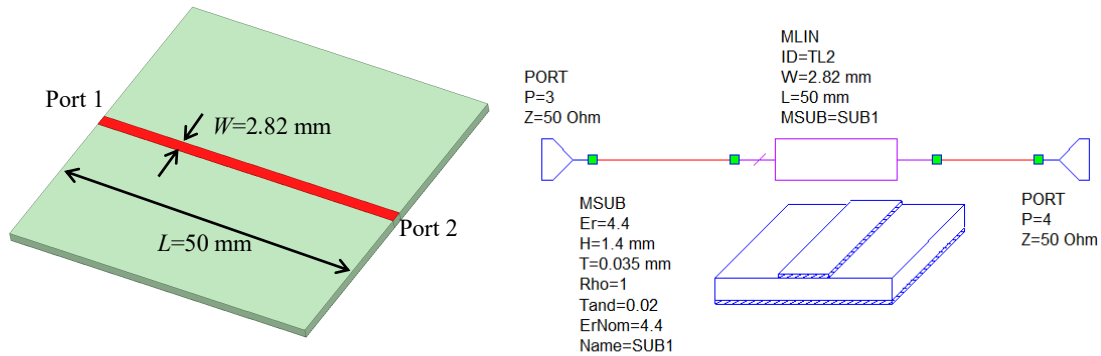


Figure 1. Microstrip line model, (left) HFSS model, (right) AWR model.

Figure 1 on the right side is the AWR model. Similarly to the HFSS ones, we model a microstrip transmission line with a length of 50 mm and a strip width of 2.82 mm through MLIN and the characteristic of the substrate itself by MSUB.

Figure 2 shows the reflection coefficient S_{11} and transmission coefficient S_{21} of the model. We see the S_{21} of both models are almost the same. For $f \leq 5$ GHz, S_{21} is better than -0.82 dB and for $f \leq 10$ GHz better than -2 dB. The reflection coefficient S_{11} fluctuates along the frequency interval, however HFSS gives a value of smaller than -20 dB, whereas AWR gives smaller than -28 dB.

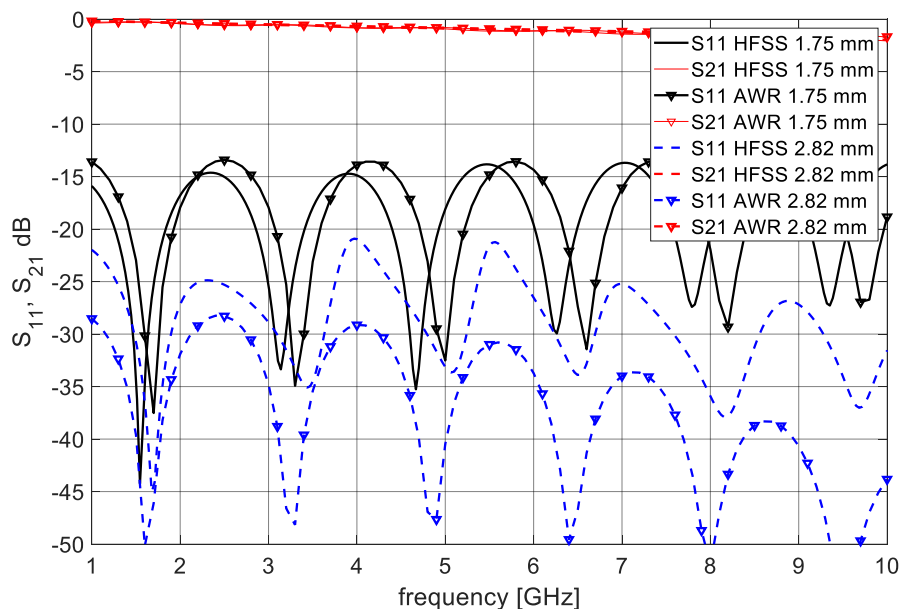


Figure 2. Comparison of reflection S_{11} and transmission coefficient S_{21} of microstrip line with strip width 2.82 mm and 1.75 mm calculated by HFSS and AWR.

Due to a rather wide strip of 2.82 mm, which could bring other problems in feeding mechanism with an SMA connector, we deliberately offer a narrower strip

width of 1.75 mm for further observation. This value is around 0.75 mm wider than the connector pin, which ensures a perfect soldering between them. Figure 2 shows the comparison of the new narrower strip. The transmission coefficient is almost unchanged. On the contrary, the reflection coefficient for 1.75 mm deteriorates significantly due to changing the characteristic impedance of the line. The value of the characteristic impedance becomes 65.1 ohm, which is unmatched with the port impedance of 50 ohm. However, the reflection coefficient still smaller than -13.5 dB.

Based on this microstrip transmission line, we observe the characteristic of an SMD resistor, an SMD capacitor and an SMD inductor. The SMDs are connected in the middle of the transmission line. This happens by defining a boundary condition of type Lumped RLC in HFSS or by inserting the associated lumped element in AWR.

We fabricated the structure under observation and did some measurement to verify the performances of the SMDs using the RS ZVA67 vector network analyzer (VNA). Before the measurement, the VNA was calibrated with the standard TOSM.

3. RESULTS AND DISCUSSION

At first, we calculate a simple microstrip transmission line in a 1.4mm thick FR4 substrate with a strip width of 1.75 mm. As described in section 2, the calculation was carried out under the software HFSS and AWR. Figure 3 shows a fabricated microstrip transmission line. For the measurement purposes, we connected an SMA connector on both sides.



Figure 3. Fabricated microstrip line in FR4 substrate with two SMA connectors.

Figure 4 gives the comparison of the computed and measured results. We see, under 5 GHz the measurement confirmed both the reflection and transmission coefficients. The measured S_{11} fluctuates in similar fashion. Only in around 6 GHz to 9.5 GHz they differ slightly. It seems, the performance of the SMA connectors deteriorates, they reflect back more energy.

The condition is very different with the transmission coefficient S_{21} for frequency bigger than 5 GHz. Although the computer program HFSS and AWR predicted increasing transmission loss with the frequency, the measurement reveals more losses occurring in the higher region. The measured transmission coefficient S_{21} decreased almost exponentially, which could be referred the attenuation factor $e^{-\alpha l}$, where α and l are attenuation constant due to FR 4 losses and transmission line length, respectively [18].

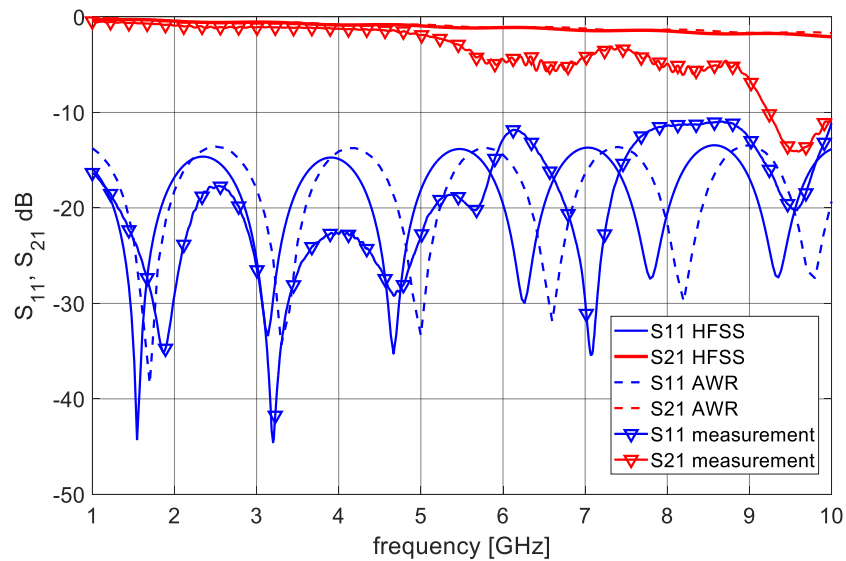


Figure 4. Comparison of reflection S_{11} and transmission coefficient S_{21} of 1.75 mm wide microstrip line.

By holding the conservation of the energy, we can calculate the loss in the circuit,

$$Loss = (1 - R - T) \times 100\%$$

Figure 5 shows the comparison of the losses calculated using the results obtained by HFSS, AWR and by measured reflection and transmission coefficient.

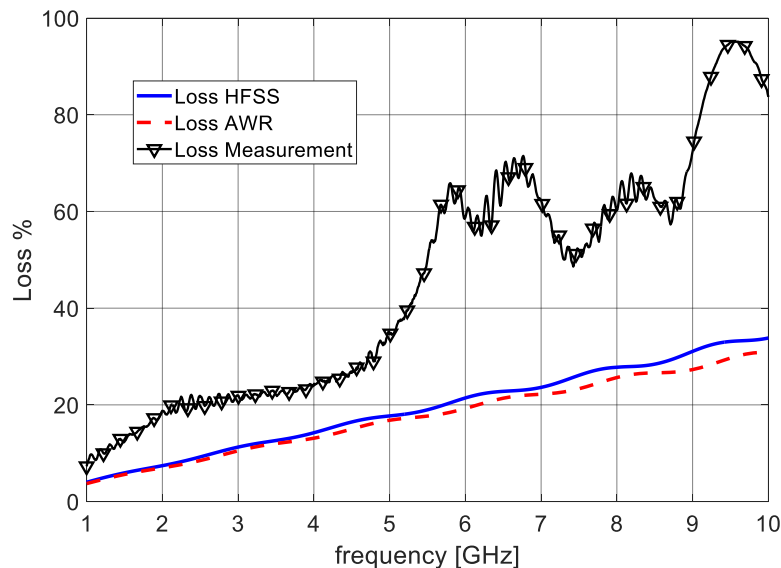


Figure 5. Comparison of losses in a 1.75mm wide microstrip line.

The calculated losses obtained by HFSS and AWR delivered almost similar results, whereas it is not the case with the measured data. We see, for frequency higher than 5.5 GHz, more than 50% of the energy disappeared. We summarized that the total higher losses in measurement are due to higher real dielectric losses in FR4 material and due to performance deterioration of the SMA connectors at higher frequencies.

For observation of SMD resistors, in HFSS we defined a rectangular patch with dimension 1.75 mm x 1.5 mm as a lumped resistor. To do that we used the feature of assigning the sheet as a boundary. Figure 6 left side shows the HFSS model, whereas the middle part of the figure gives the AWR model, just as in the transmission line model, here we split the transmission line into two parts and connecting the lumped model of resistance RES in the middle. Figure 6 shows also a photograph of the soldered SMD resistor in the microstrip line.

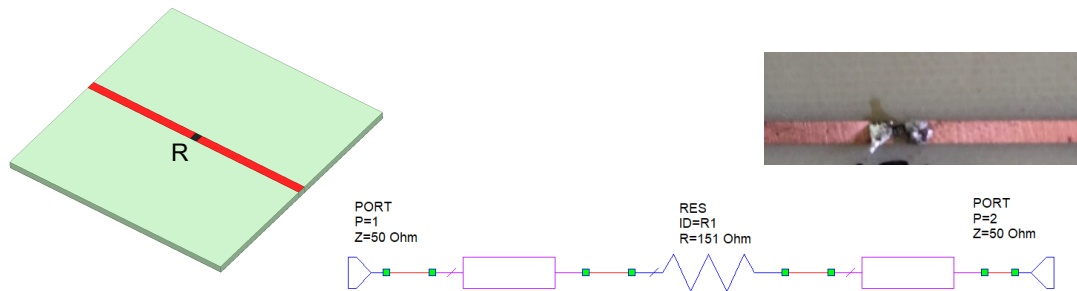


Figure 6. SMD resistor of 151.0 ohm, (left) HFSS model, (middle) AWR model, (right) fabricated circuit.

The comparison of the simulated and measured reflection and transmission coefficient for SMD resistor is given in Figure 7. We see again for up to around 5 GHz, the results are almost the same, whereas for higher frequencies they differ mainly due to higher loss in the measurements.

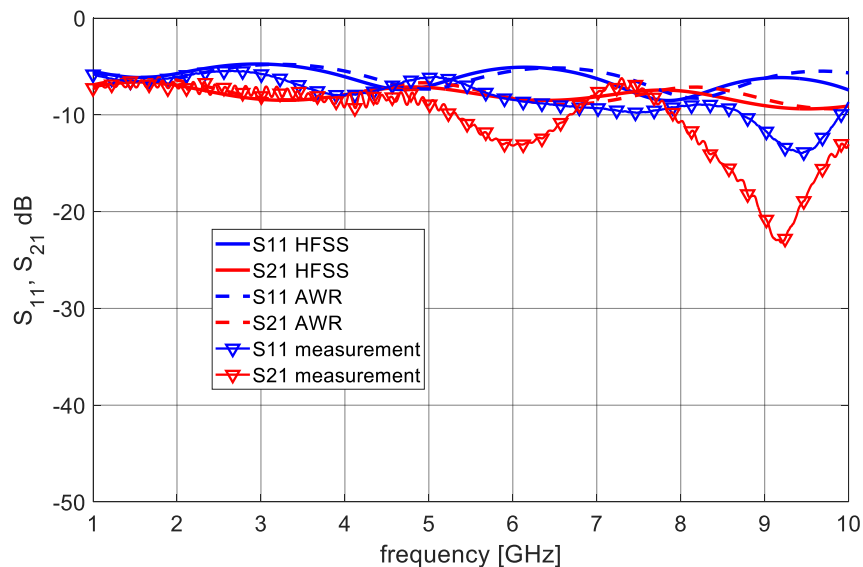


Figure 7. Comparison of reflection S_{11} and transmission coefficient S_{21} of 151-ohm SMD resistance on 1.75mm wide microstrip line.

The model for SMD capacitor is given in Figure 8 left and middle side for HFSS and AWR respectively. The photograph of the solder SMD capacitor is given in Figure 8 on right side.

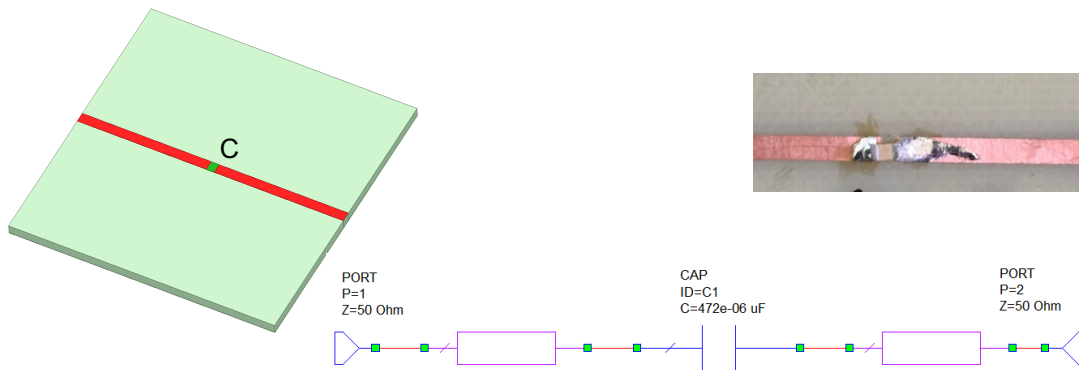


Figure 8. SMD capacitor of 472 pF, (left) HFSS model, (middle) AWR model, (right) fabricated circuit.

Figure 9 gives the comparison of the calculated and measured results. We see, the measured reflection coefficient is very small for frequency smaller than 6 GHz, the measured transmission coefficient is almost the same like the calculated ones. And again here, for higher frequencies the measurement shows too higher losses, which confirms the finding for the transmission line case.

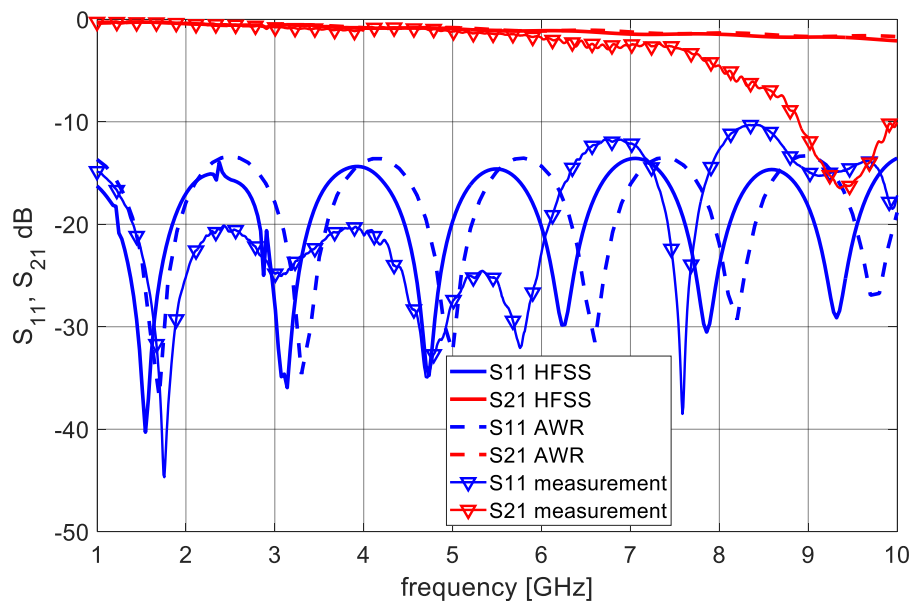


Figure 9. Comparison of reflection S_{11} and transmission coefficient S_{21} of 472 pF SMD capacitance on 1.75mm wide microstrip line.

Lastly, we model for an SMD inductor, in this case we soldered a Samsung SMD inductor of type CIL31Y100KN with an inductance of $10 \mu\text{H}$. Figure 10 gives the calculation model for HFSS and AWR, and also the photograph of the soldered SMD inductor in the microstrip.

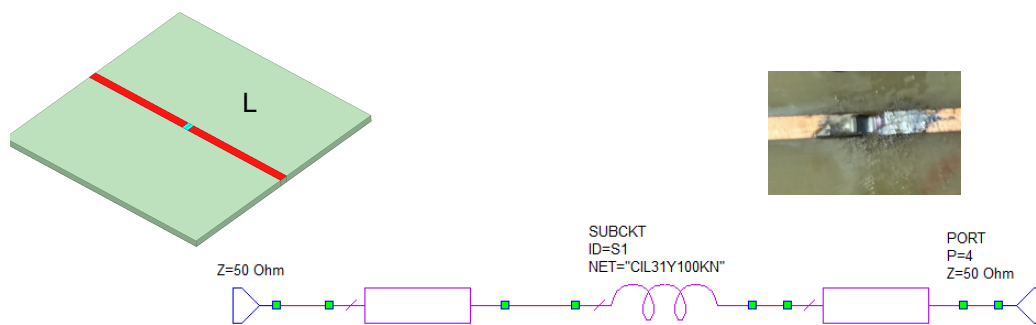


Figure 10. SMD inductance $10 \mu\text{H}$ (Samsung CIL31Y100KN), (left) HFSS model, (middle) AWR model, (right) fabricated circuit.

We see in Figure 11; the red and blue solid lines differ from other representative comparison. Whereas the dashed and triangle curves are at least up to 7 GHz are similar. HFSS model fails to model the SMD inductance. Probably, just a lumped inductance model of $10 \mu\text{H}$ in HFSS cannot represent the actual SMD inductor. On the other hand, the AWR model gives reflection and transmission characteristics which show a very good similarity to the measured reflection and transmission coefficient up to 7 GHz. The model is available in the component library in AWR under the name Samsung CIL31Y100KN.

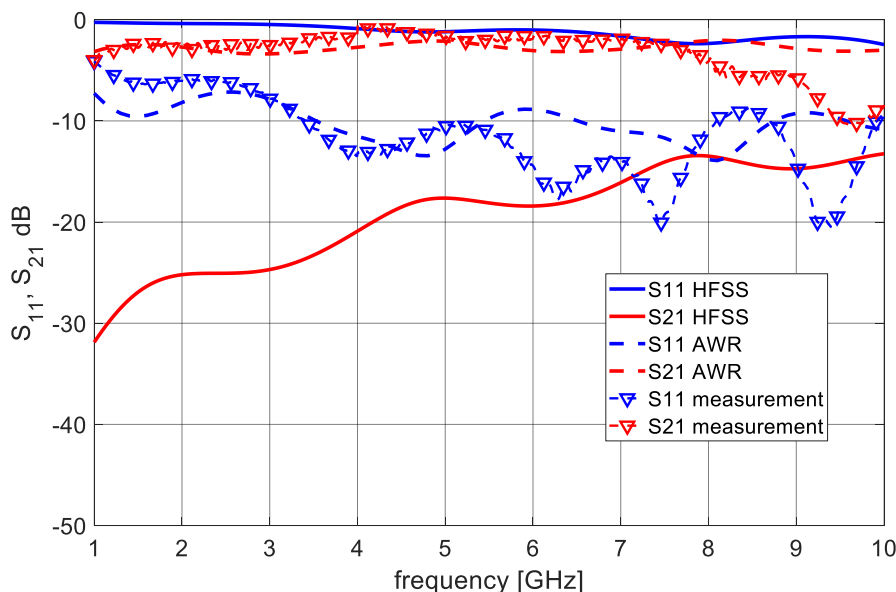


Figure 11. Comparison of reflection S_{11} and transmission coefficient S_{21} of $10 \mu\text{H}$ SMD inductance on 1.75mm wide microstrip line.

4. CONCLUSION

The computer program HFSS and AWR give almost the same results for all cases except for the SMD inductance. In this way we can rely on the computational modeling. The reflection and transmission coefficient of a 1.4mm thick microstrip line were verified by measurement with a very good similarity up to 5 GHz. The

comparison of the simulated and measured reflection and transmission coefficient for SMD resistor is almost the same for up to around 5 GHz, whereas for SMD capacitor for up to around 6 GHz and for SMD inductor for up to around 7 GHz.

ACKNOWLEDGMENT

We would like to thank Universitas Mercu Buana for the support of laboratory equipment and the Kemendikbudristek (research schema PTM with the contract number 105/E5/PG.02.00.PL/2024) for financial support the research.

REFERENCES

- [1] C. Roy and K. Wu, "A Review of Electromagnetics-Based Microwave Circuit Design Optimization," *IEEE Microwave*, vol. 25, no. 7, pp. 16–40, Jul. 2024, doi: 10.1109/MMM.2024.3387036.
- [2] J. E. Rayas-Sánchez et al., "Microwave Modeling and Design Optimization: The Legacy of John Bandler," *IEEE Trans. Microwave Theory Techn.*, pp. 1–0, 2024, doi: 10.1109/TMTT.2024.3437198.
- [3] J. E. Rayas-Sanchez, S. Koziel, and J. W. Bandler, "Advanced RF and Microwave Design Optimization: A Journey and a Vision of Future Trends," *IEEE J. Microw.*, vol. 1, no. 1, pp. 481–493, Jan. 2021, doi: 10.1109/JMW.2020.3034263.
- [4] Y. Yu et al., "State-of-the-Art: AI-Assisted Surrogate Modeling and Optimization for Microwave Filters," *IEEE Trans. Microwave Theory Techn.*, vol. 70, no. 11, pp. 4635–4651, Nov. 2022, doi: 10.1109/TMTT.2022.3208898.
- [5] F. Feng, W. Na, J. Jin, J. Zhang, W. Zhang, and Q.-J. Zhang, "Artificial Neural Networks for Microwave Computer-Aided Design: The State of the Art," *IEEE Trans. Microwave Theory Techn.*, vol. 70, no. 11, pp. 4597–4619, Nov. 2022, doi: 10.1109/TMTT.2022.3197751.
- [6] G. Macchiarella and S. Tamiazzo, "Cooking Microwave Filters: Is Synthesis Still Helpful in Microwave Filter Design?," *IEEE Microwave*, vol. 21, no. 3, pp. 20–33, Mar. 2020, doi: 10.1109/MMM.2019.2958148.
- [7] W. Zhang et al., "Advanced Parallel Space-Mapping-Based Multiphysics Optimization for High-Power Microwave Filters," *IEEE Trans. Microwave Theory Techn.*, vol. 69, no. 5, pp. 2470–2484, May 2021, doi: 10.1109/TMTT.2021.3065972.
- [8] C.-Y. Zhuang, D.-B. Lin, T.-Y. Lee, and F.-Y. Hsieh, "Novel Equivalent Circuit Model for Dual-Band Series-Unified Absorptive Common-Mode Filter," *IEEE Trans. Electromagn. Compat.*, pp. 1–4, 2024, doi: 10.1109/TEMC.2024.3432147.
- [9] M. M. Zargar, A. Rajput, and K. Saurav, "Equivalent Circuit-Aided Miniaturized High-Q Frequency-Selective Resorber," *IEEE Lett. on Electromagn. Compat. Pract. and Appl.*, vol. 6, no. 3, pp. 96–101, Sep. 2024, doi: 10.1109/LEMCPA.2024.3424390.
- [10] M. Pérez-Escribano, S. Moreno-Rodríguez, C. Molero, J. F. Valenzuela-Valdés, P. Padilla, and A. Alex-Amor, "Analytical Framework to Model Reconfigurable Metasurfaces Including Lumped Elements," *IEEE Trans. Circuits Syst. II*, vol. 71, no. 4, pp. 1784–1788, Apr. 2024, doi: 10.1109/TCSII.2023.3330318.
- [11] J. Chen, X.-M. Li, and R.-X. Wu, "Equivalent Circuit Model of Lumped Elements Retrieved from Measured S-Parameters of Microstrip Line in Frequency Range 0.5-5GHz," in *2020 IEEE MTT-S International Wireless Symposium (IWS)*, Shanghai, China: IEEE, Sep. 2020, pp. 1–3. doi: 10.1109/IWS49314.2020.9360005.
- [12] I. J. Bahl, *Lumped elements for RF and microwave circuits*, Second edition. in *Artech House microwave library*. Boston London: ARTECH HOUSE, 2023.
- [13] Y. Xiao, Z. Zhou, M. Sheng, and Q. Zhou, "A Combination Method for Impedance Extraction of SMD Electronic Components Based on Full-Wave Simulation and De-Embedding Technique," *IEICE Trans. Fundamentals*, vol. E107.A, no. 8, pp. 1345–1354, Aug. 2024, doi: 10.1587/transfun.2023EAP1102.
- [14] J. Anderson, M. Fahd, "High frequency modeling of SMD resistors," M.S. Thesis, Dept. of

- Microtechnology and Nanoscience, Chalmers University of Technology, Gothenburg, Sweden, 2024. Accessed on: Sept., 11, 2024. Available: <https://odr.chalmers.se/items/81b9a294-7079-4cca-bef4-9e2f8759393f>.
- [15] L. Dunleavy, "Moving Beyond S-Parameter Files: Advanced Scalable and 3D EM Models for Passive Devices," in 2019 IEEE International Conference on Microwaves, Antennas, Communications and Electronic Systems (COMCAS), Tel-Aviv, Israel: IEEE, Nov. 2019, pp. 1–7. doi: 10.1109/COMCAS44984.2019.8958187.
- [16] ANSYS HFSS 2024. Accessed on: Sept., 9, 2024. <https://www.ansys.com/products/electronics/ansys-hfss>.
- [17] AWR Cadence 2024. Accessed on: Sept., 9, 2024. https://www.cadence.com/ko_KR/home/tools/system-analysis/rf-microwave-design.html.
- [18] M. Alaydrus, Transmission Lines in Telecommunication. Graha Ilmu, 2009.